

## Electronic structure and optical transition energies of the $U$ center in alkaline-earth fluorides\*

L. E. Oliveira, B. Maffeo, and H. S. Brandi

*Departamento de Física, Pontifícia Universidade Católica do Rio de Janeiro, Rua Marquês de S. Vicente 225, Gávea 20.000, Rio de Janeiro, Brazil*

M. L. de Siqueira

*Departamento de Física-Icex, Universidade Federal de Minas Gerais, Caixa Postal 1621, 30.000 Belo Horizonte, Brazil*

(Received 19 March 1976; revised manuscript received 10 December 1976)

The self-consistent-field multiple-scattering method in the  $X\alpha$  approximation is used to calculate the electronic structure and the optical transition energies of the  $U$  center in  $\text{CaF}_2$ ,  $\text{SrF}_2$ , and  $\text{BaF}_2$ .

### I. INTRODUCTION

The model for the  $U$  center in ionic crystals has been unambiguously defined by extensive experimental work and consists of an  $\text{H}^-$  ion substitutionally located at an anion vacancy. The phonon spectrum and the optical properties of these crystals are changed when this defect is created. Localized vibrational modes which are strongly infrared active and a characteristic optical absorption band in the uv region are present. Using optical techniques (Raman scattering, infrared, and uv absorption), several researchers have studied these properties in alkali halides<sup>1-7</sup> and in alkaline-earth fluorides.<sup>8-11</sup>

The  $U$  center is one of the simplest color centers which can be produced in ionic crystals and for this reason it has been the subject of many theoretical calculations. Related to the optical absorption band a number of papers concern the calculation of the electronic states of the  $\text{H}^-$  ion in alkali halides,<sup>12-17</sup> both in  $\text{NaCl}$ - and  $\text{CsCl}$ -type structures, and in alkaline-earth fluorides.<sup>16-18</sup> Except for the work of Wood and Öpik<sup>14</sup> all theoretical treatments assume the  $\text{H}^-$  ion placed in a point-ion lattice representing the host crystal; the optical band was associated with the difference in energy between the  $\text{H}^-$   $^1S(1s^2)$  and  $^1P(1s2p)$  states, and the results are systematically smaller than the experimental ones. Bennett<sup>16,17</sup> presents a detailed discussion about the limitations of the point-ion model. These are basically the neglect of the finite size of the ions neighboring the  $\text{H}^-$  and of polarization effects. Wood and Öpik<sup>14</sup> calculated the electronic structure of the  $U$  center in  $\text{KCl}$ ,  $\text{KBr}$ , and  $\text{KI}$  for the ground and first-excited states using a model in which the interactions with the first-nearest-neighbor ions are taken into account in detail and all other ions are treated as point charges, their results being significantly better than those obtained by the simplest point-ion model. In this same work,<sup>14</sup> a second more complex model which involves within cer-

tain approximations the electronic structure of all ions and polarization effects is used for calculations of the electronic structure, optical absorption, and lattice relaxation of the  $U$  center in  $\text{KCl}$ , obtaining in this case significant polarization effects even in the ground state.

In the present work we calculate the electronic structure and optical absorption transitions of the  $U$  center in  $\text{CaF}_2$ ,  $\text{SrF}_2$ , and  $\text{BaF}_2$ . In the previous calculations,<sup>16-18</sup> Singh *et al.*<sup>18</sup> have used variational wave functions containing two adjustable parameters, whereas Bennett<sup>16,17</sup> solved numerically the Hartree-Fock-Slater equations for the two electron orbitals of  $\text{H}^-$ , allowing relaxation of its first neighbors. Although Bennett<sup>16,17</sup> uses a more "flexible" scheme than that used by Singh *et al.*,<sup>18</sup> the latter results are in better agreement with experiment. This indicates that it is not possible to describe realistically the  $U$  center within the point-ion approximation and emphasizes a need for models involving detailed treatment of the finite size of neighboring ions and electronic polarization, as were to some extent used by Wood and Öpik.<sup>14</sup> It is well known that the inclusion of electronic polarization is extremely difficult in an *ab initio* calculation. Certainly an important improvement in the description of the electronic structure of the defect could be obtained by using self-consistent molecular orbitals from a linear combination of atomic orbitals (LCAO-MO SCF), but such a calculation has not yet been done for the case of alkaline-earth fluorides. For the  $F$  center in  $\text{LiF}$  this scheme has been successfully used by Chaney and Lin.<sup>19</sup> Recently, Yu *et al.*<sup>20,21</sup> used the SCF-multiple-scattering (MS) method in the  $X\alpha$  approximation ( $\text{MSX}\alpha$ ) to study the  $U$  center in several alkali halides obtaining for the optical transition a good agreement with experiment. Clementi *et al.*<sup>22</sup> have shown that LCAO-MO calculations are competitive with  $\text{MSX}\alpha$  in terms of computer time and are potentially more accurate.

The  $\text{MSX}\alpha$  method has been extensively discussed

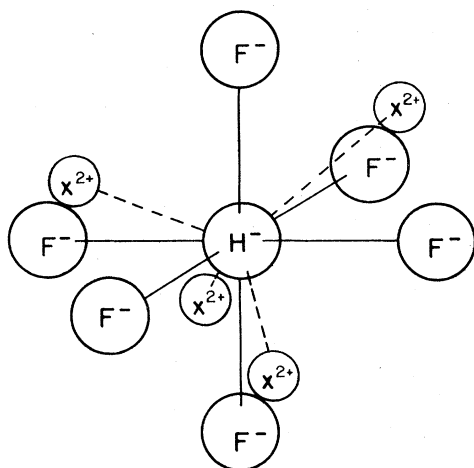


FIG. 1. Complex chosen as a model for the  $U$  center in  $\text{CaF}_2$ ,  $\text{SrF}_2$ , and  $\text{BaF}_2$ .

by several authors that applied it to many molecular systems.<sup>23-28</sup> This is a very "flexible" computing method which takes into account spin polarization (within a mono-electronic scheme) together with the possibility of inclusion of a great number of ions reflecting the proper local symmetry of the physical system. This scheme was used in the present paper.

In Sec. II we describe the basic assumptions of the present calculations; results and discussion concerning the electronic structure and optical absorption transitions are presented in Sec. III; the conclusions of this work are in Sec. IV.

## II. DETAILS OF THE CALCULATIONS

We have used the  $\text{MSX}\alpha$  method in the usual muffin-tin approximation which is believed to be appropriate in describing complexes with a predominant degree of ionic binding as we expect to be the case for the  $U$  center in alkaline-earth fluorides. In this work the structure of the defect is approximated by the complex shown in Fig. 1, which has  $T_d$  symmetry. Within these approximations the potentials and charge densities in the spheres containing the substitutional  $\text{H}^-$  ion and the ions surrounding it are spherically averaged. Outside the whole complex the potential and charge density are

also spherically averaged. For the interspheres region, volume averages of the charge density and potential are used, giving a constant value for the final interspheres potential.

The choice of the muffin-tin spheres radii is usually made respecting the constraint imposed by the lattice parameter and in such manner as to minimize the constant potential region. The latter feature is generally achieved by imposing the condition that all the spheres be tangent to each other and, in order to have a sufficiently realistic description of the physical system, that each sphere radius is chosen to be proportional to the tabulated ionic radius of the corresponding element.<sup>29</sup> For the complex shown in Fig. 1 these conditions cannot be satisfied simultaneously and three different choices for the muffin-tin scheme are possible, namely, (i) first cluster: the spheres associated with  $\text{H}^-$  and  $\text{F}^-$  are tangent, their radii being proportional to the corresponding ionic radii; the cation spheres are tangent to the  $\text{H}^-$  sphere; (ii) second cluster: the spheres associated with  $\text{F}^-$  and to the cations are tangent, their radii being proportional to the corresponding ionic radii; the  $\text{H}^-$  sphere is tangent to the cation spheres; (iii) third cluster: the spheres associated with  $\text{H}^-$  and to the cations are tangent, their radii being proportional to the corresponding ionic radii; the  $\text{F}^-$  spheres are tangent to the  $\text{H}^-$  sphere for  $\text{CaF}_2$  and  $\text{SrF}_2$ , whereas they are tangent to the cation spheres for  $\text{BaF}_2$ .

The smallest possible radius avoiding overlap with the inner spheres is always chosen as the radius of the outer sphere. Tables I and II present all the data concerning this discussion. Figure 2 shows the possible choices for the muffin-tin scheme in the case of  $\text{BaF}_2$ , for which the differences are more apparent as compared to the other fluorides.

It is clear that, for the complex chosen in the present work to represent the  $U$  center in the three alkaline-earth fluorides, the specification of the muffin-tin scheme is not unique. As it is not strongly evident which of the three possible clusters is the best representation for the defect and we were interested in investigating the dependence of the theoretical results on the muffin-tin scheme,

TABLE I. Muffin-tin radii ( $R$ ) used in the calculations. Values are all in atomic units.

	First cluster			Second cluster			Third cluster		
	$\text{CaF}_2$	$\text{SrF}_2$	$\text{BaF}_2$	$\text{CaF}_2$	$\text{SrF}_2$	$\text{BaF}_2$	$\text{CaF}_2$	$\text{SrF}_2$	$\text{BaF}_2$
$R_{\text{out}}$	7.558	8.023	8.576	7.728	8.060	8.388	7.606	8.216	8.574
$R_{\text{cation}}$	1.701	1.806	1.930	1.908	2.170	2.546	1.750	1.999	2.361
$R_{\text{F}^-}$	2.393	2.540	2.715	2.563	2.577	2.527	2.442	2.733	2.714
$R_{\text{H}^-}$	2.770	2.941	3.144	2.563	2.577	2.527	2.722	2.749	2.714

TABLE II. Ionic radii ( $R'$ ). Values are all in atomic units.

$R'$ ( $\text{Ca}^{2+}$ )	$R'$ ( $\text{Sr}^{2+}$ )	$R'$ ( $\text{Ba}^{2+}$ )	$R'$ ( $\text{F}^-$ )	$R'$ ( $\text{H}^-$ )
1.871	2.117	2.533	2.514	2.911

calculations have been done for the first two. Table I shows that the muffin-tin scheme associated with the third cluster is described by parameters with values in general lying between those which describe the first and second; therefore we expect that our calculations will properly give the relevant check for the method.

The complex considered has a total positive charge of +1 and in order to stabilize it we replace the potential due to the rest of the crystal by an uniformly distributed charge of -1 on the outer sphere ("Watson sphere"<sup>30</sup>).

The nonlocal correlation potential in the Hartree-Fock equations is replaced by the  $X\alpha$  statistical exchange potential.<sup>31,32</sup> We have used the  $\alpha$  values calculated by Schwarz<sup>33</sup> for calcium, strontium, and fluorine. The value of  $\alpha$  used for barium was obtained by linear extrapolation and for the  $\text{H}^-$  ion from a spin-polarized calculation done for hydrogen.<sup>34,35</sup> Following the suggestion of Yu *et al.*<sup>21</sup> we have used a weighted average  $\alpha$  value for the interspheres and outer regions. The electronic structure calculations were done in both spin-nonpolarized and spin-polarized Hartree-

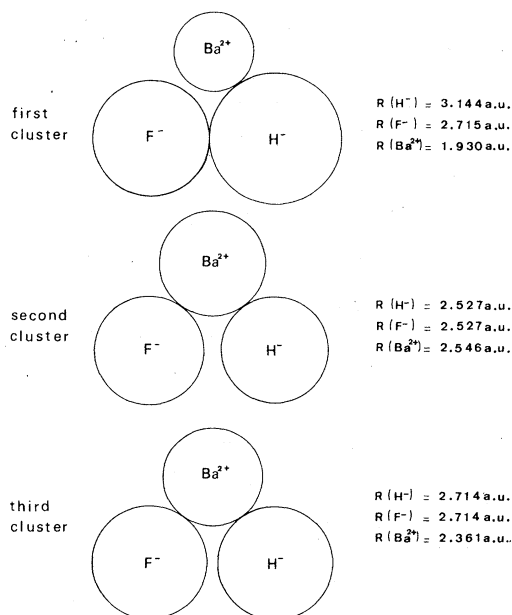


FIG. 2. Bidimensional schematic in-scale-representation of the clusters for  $\text{BaF}_2$ . Muffin-tin radii ( $R$ ).

Fock schemes; as expected they are equivalent since the defect presents a closed shell structure. In the evaluation of optical transitions we have used the concept of transition state<sup>36</sup> and no significant modification was obtained using the spin-polarized scheme.

All calculations have been done using, for fluorine and cation spheres, partial wave expansions with  $l=0$  and 1, and for  $\text{H}^-$ ,  $l=0, 1, 2$ , and 3. For the first cluster, in the case of  $\text{CaF}_2$ , we also included  $l=2$  for the fluorine and cation spheres obtaining essentially the same results.

Self-consistency in the energy levels was carried out up to the fourth decimal in all cases.

### III. RESULTS AND DISCUSSION

#### A. Electronic structure of the $U$ center in $\text{CaF}_2$ , $\text{SrF}_2$ , and $\text{BaF}_2$

The one-electron energy levels (corresponding to the ground-state configuration) which are not essentially atomic are presented in Figs. 3-5 for  $\text{CaF}_2$ ,  $\text{SrF}_2$ , and  $\text{BaF}_2$ , respectively. The results are shown for the first and second clusters, in the spin-non-polarized scheme. In all these figures the two highest energy levels,  $5a_1$  and  $7t_2$ , are associated to unoccupied states delocalized inside the cluster. The occupied  $3a_1$  and  $4a_1$  states are

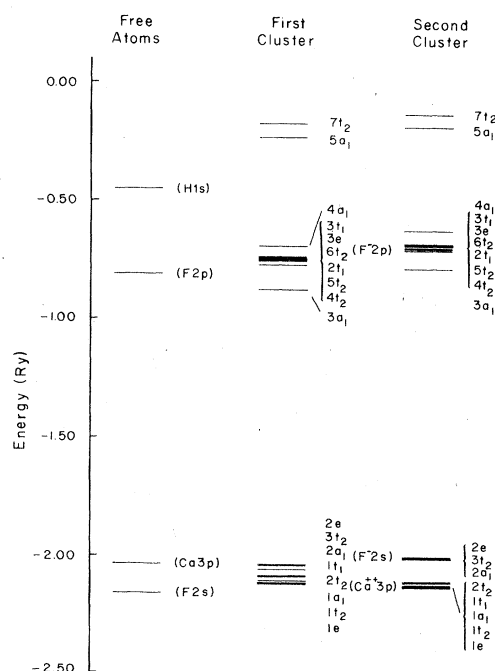


FIG. 3. One-electron energy levels from the ground-state calculation of the  $U$  center in  $\text{CaF}_2$ . Also shown for comparison are the corresponding SCF  $X\alpha$  energy levels of the free atoms.

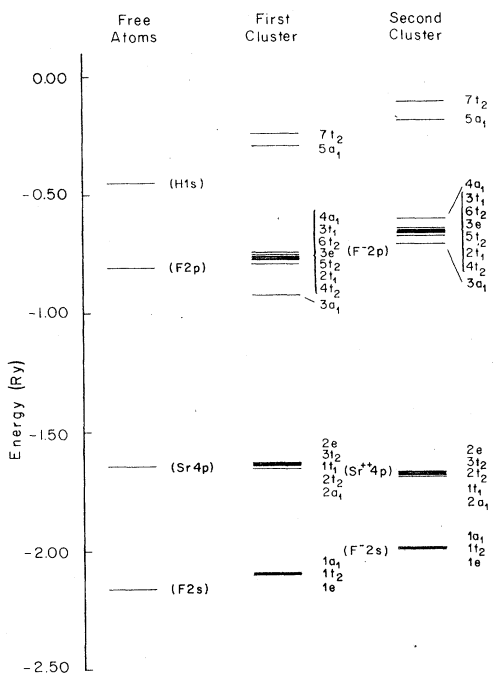


FIG. 4. One-electron energy levels from the ground-state calculation of the  $U$  center in  $\text{SrF}_2$ . Also shown for comparison are the corresponding SCF  $X\alpha$  energy levels of the free atoms.

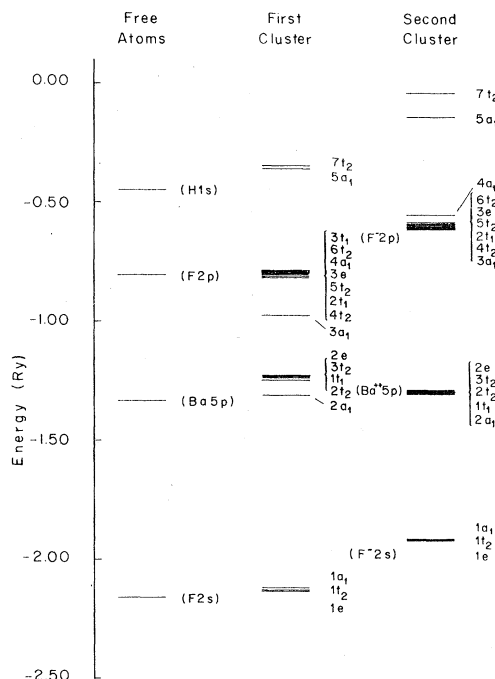


FIG. 5. One-electron energy levels from the ground-state calculations of the  $U$  center in  $\text{BaF}_2$ . Also shown for comparison are the corresponding SCF  $X\alpha$  energy levels of the free atoms.

basically a mixture of hydrogen and neighboring fluorine atomic states as can be seen from the percentual charge distributions presented in Table III; the other occupied states have a predominant atomic nature which is identified in these figures inside parentheses.

The percentual charge distribution shown in Table III indicates that  $3a_1$  is mostly hydrogenic while  $4a_1$  is fluorinelike, except for  $\text{BaF}_2$  in the second cluster calculation where these characteristics are interchanged. Another difference between the first- and second-cluster calculations, for the three crystals, can be observed in Table

TABLE III. Percentual amount of charge inside the hydrogen and fluorine spheres arising from the wave function associated to the energy levels  $3a_1$  and  $4a_1$ . Fluorine charge is obtained by adding the charge in each of the six spheres around the  $\text{H}^-$  ion.

	First cluster			Second cluster		
	$\text{CaF}_2$	$\text{SrF}_2$	$\text{BaF}_2$	$\text{CaF}_2$	$\text{SrF}_2$	$\text{BaF}_2$
$3a_1(\text{H}^-)$	61%	77%	67%	47%	46%	25%
$3a_1(\text{F}^-)$	26%	10%	1%	40%	39%	60%
$4a_1(\text{H}^-)$	28%	12%	3%	39%	39%	58%
$4a_1(\text{F}^-)$	67%	83%	92%	55%	55%	33%

IV where the percentual charge distributions of the "cation"  $a_1$  level are significantly dependent on the choice of the cluster. These are the most striking features which distinguish the results obtained using the two muffin-tin schemes chosen; of course, as can be seen in Figs. 3-5, there are also quantitative differences between the one-electron eigenvalues corresponding to each of the two calculated ground-state configurations.

Table V presents the total charges in each region of the clusters. It shows that the charges in the outersphere and interspheres regions are always small compared with the total charge of the

TABLE IV. Percentual amount of charge inside the hydrogen, fluorine, and cation spheres arising from the wave function associated to the "cation" energy level  $a_1$  ( $1a_1$  for  $\text{CaF}_2$  and  $2a_1$  for  $\text{SrF}_2$  and  $\text{BaF}_2$ ). Fluorine and cation charges are obtained by adding the charges in each of the corresponding spheres around the  $\text{H}^-$  ion.

	First cluster			Second cluster		
	$\text{CaF}_2$	$\text{SrF}_2$	$\text{BaF}_2$	$\text{CaF}_2$	$\text{SrF}_2$	$\text{BaF}_2$
$a_1(\text{H}^-)$	1%	5%	27%	1%	2%	3%
$a_1(\text{F}^-)$	31%	1%	2%	5%	1%	1%
$a_1(\text{cation})$	58%	75%	46%	87%	87%	83%

TABLE V. Total charge for different regions of the clusters.

	First cluster			Second cluster		
	CaF <sub>2</sub>	SrF <sub>2</sub>	BaF <sub>2</sub>	CaF <sub>2</sub>	SrF <sub>2</sub>	BaF <sub>2</sub>
H <sup>+</sup>	2.01	2.12	2.37	1.86	1.83	1.78
F <sup>-</sup>	9.42	9.51	9.60	9.57	9.57	9.53
Cation	17.07	34.49	51.55	17.43	35.27	53.13
Intersphere charge	7.12	8.78	11.73	4.91	5.58	6.40
Outersphere charge	0.11	0.09	0.07	0.10	0.10	0.11

cluster which is a good indication that these muffin-tin approximations are reasonable.

#### B. Optical transitions for the $U$ center in CaF<sub>2</sub>, SrF<sub>2</sub>, and BaF<sub>2</sub>

In Table VI the theoretical results obtained by Bennett<sup>16,17</sup> and Singh *et al.*<sup>18</sup> are presented together with the experimental results concerning the peak position and halfwidth of the  $U$ -center absorption band in CaF<sub>2</sub>, SrF<sub>2</sub>, and BaF<sub>2</sub>. These authors, using a point-ion model, associated the  $U$ -band to the  $^1S(1s^2) \rightarrow ^1p(1s2p)$  transition in the H<sup>-</sup> ion.

In the present work we have calculated all the symmetry allowed transitions to the unoccupied  $5a_1$  and  $7t_2$  levels from the occupied group of one-electron states with energy immediately below those two. All the results are presented in Tables VII–IX where we compare the values obtained using the transition-state concept or simply taking the difference associated with the eigenvalues corresponding to the levels involved in the transition. A pictorial comparison between experiment and the results of the transition-state calculations (except the  $3a_1 \rightarrow 7t_2$  transition) is presented in Figs. 6–8 where the  $U$ -band is simulated by a Gaussian (the only experimental results available are the halfwidth and the peak position of the optical band<sup>11</sup>) and the vertical bars placed on the upper and lower

sides of the horizontal (energy) axis correspond to the transitions evaluated using the first and second clusters, respectively. In these same figures we also represent the results of Bennett<sup>16,17</sup> and of Singh *et al.*<sup>18</sup> by points and crosses, respectively. Of course, in this type of comparison, we are disregarding the role of electron-phonon interaction which would associate a certain width to each of the calculated transitions.

It is striking that for CaF<sub>2</sub> and SrF<sub>2</sub>, in both cluster calculations, all allowed transitions, except  $3a_1 \rightarrow 7t_2$ , lie inside the experimental band. The present model for the defect associates the  $U$ -band to transitions arising from a group of almost degenerate states, basically related with the  $2p$  F<sup>-</sup> band, to the unoccupied  $5a_1$  and  $7t_2$  states; this interpretation is in contrast with all the above mentioned calculations for this kind of defect in these crystals, which associate the  $U$  band to a single transition in H<sup>-</sup>.

The calculations for BaF<sub>2</sub> still show a reasonable agreement with experiment if one considers that the appropriate muffin-tin scheme representing the  $U$  center is that of the first cluster. Also in this case, assuming the same type of transitions, several of them lie in the energy range of the experimental band. This type of agreement is not obtained if we use the second-cluster description for the defect.

TABLE VI. Lattice parameter ( $\text{\AA}$ ), experimental halfwidth (eV), experimental and theoretical peak position (eV) of the  $U$  band.

	Lattice parameter Ref. 37	Halfwidth (expt.) Ref. 11	Peak position (expt.) Ref. 11	Peak position (theor.) Ref. 18	Peak position (theor.) Refs. 16 and 17
CaF <sub>2</sub>	5.463	0.493	7.65	6.82	6.42
SrF <sub>2</sub>	5.800	0.420	7.04	6.37	5.90
BaF <sub>2</sub>	6.200	0.367	6.00	5.89	5.47

TABLE VII. Theoretical optical transition energies (eV) for  $U$  center in  $\text{CaF}_2$ .

$\text{CaF}_2$ Optical transition	First cluster		Second cluster	
	Integer occupation	Transition state	Integer occupation	Transition state
$\epsilon(7t_2)-\epsilon(3a_1)$	9.48	10.18	8.92	10.59
$\epsilon(7t_2)-\epsilon(4t_2)$	8.10	8.11	7.98	8.18
$\epsilon(7t_2)-\epsilon(5t_2)$	7.88	7.90	7.79	8.02
$\epsilon(7t_2)-\epsilon(2t_1)$	7.85	7.88	7.77	8.00
$\epsilon(7t_2)-\epsilon(6t_2)$	7.72	7.76	7.65	7.89
$\epsilon(7t_2)-\epsilon(3e)$	7.71	7.75	7.64	7.89
$\epsilon(7t_2)-\epsilon(3t_1)$	7.65	7.69	7.58	7.82
$\epsilon(5a_1)-\epsilon(4t_2)$	7.32	7.36	7.24	7.48
$\epsilon(5a_1)-\epsilon(5t_2)$	7.10	7.15	7.05	7.31
$\epsilon(7t_2)-\epsilon(4a_1)$	7.04	7.10	6.76	7.21
$\epsilon(5a_1)-\epsilon(6t_2)$	6.94	7.01	6.91	7.19

TABLE VIII. Theoretical optical transition energies (eV) for  $U$  center in  $\text{SrF}_2$ .

$\text{SrF}_2$ Optical transition	First cluster		Second cluster	
	Integer occupation	Transition state	Integer occupation	Transition state
$\epsilon(7t_2)-\epsilon(3a_1)$	9.34	9.92	8.20	10.09
$\epsilon(7t_2)-\epsilon(4t_2)$	7.49	7.54	7.60	7.80
$\epsilon(7t_2)-\epsilon(2t_1)$	7.31	7.38	7.46	7.68
$\epsilon(7t_2)-\epsilon(5t_2)$	7.28	7.35	7.42	7.64
$\epsilon(7t_2)-\epsilon(3e)$	7.16	7.24	7.31	7.55
$\epsilon(7t_2)-\epsilon(6t_2)$	7.15	7.23	7.30	7.53
$\epsilon(7t_2)-\epsilon(3t_1)$	7.05	7.13	7.21	7.44
$\epsilon(7t_2)-\epsilon(4a_1)$	6.91	6.90	6.70	7.09
$\epsilon(5a_1)-\epsilon(4t_2)$	6.80	6.87	6.78	7.02
$\epsilon(5a_1)-\epsilon(5t_2)$	6.60	6.68	6.60	6.86
$\epsilon(5a_1)-\epsilon(6t_2)$	6.47	6.56	6.48	6.76

TABLE IX. Theoretical optical transition energies (eV) for  $U$  center in  $\text{BaF}_2$ .

$\text{BaF}_2$ Optical transition	First cluster		Second cluster	
	Integer occupation	Transition state	Integer occupation	Transition state
$\epsilon(7t_2)-\epsilon(3a_1)$	8.51	8.55	7.89	9.51
$\epsilon(7t_2)-\epsilon(4t_2)$	6.42	6.68	7.85	7.75
$\epsilon(7t_2)-\epsilon(2t_1)$	6.31	6.59	7.76	7.69
$\epsilon(7t_2)-\epsilon(5t_2)$	6.22	6.49	7.66	7.59
$\epsilon(7t_2)-\epsilon(3e)$	6.13	6.41	7.58	7.52
$\epsilon(5a_1)-\epsilon(4t_2)$	6.25	6.35	6.41	6.65
$\epsilon(7t_2)-\epsilon(6t_2)$	6.07	6.34	7.54	7.47
$\epsilon(7t_2)-\epsilon(4a_1)$	6.09	6.29	7.01	7.23
$\epsilon(7t_2)-\epsilon(3t_1)$	5.93	6.20	7.42	7.36
$\epsilon(5a_1)-\epsilon(5t_2)$	6.06	6.16	6.22	6.48
$\epsilon(5a_1)-\epsilon(6t_2)$	5.91	6.01	6.10	6.37

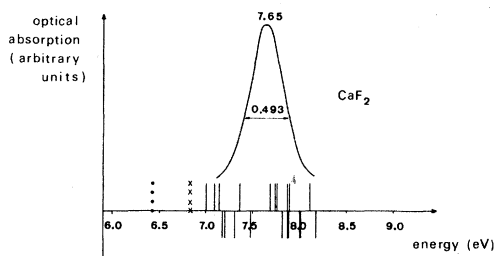


FIG. 6. Comparison between experiment and the results of the transition-state calculations for  $\text{CaF}_2$ . Vertical bars in the upper and lower sides of horizontal axis correspond to first- and second-cluster calculations, respectively. Also shown are the theoretical results of Bennett (Ref. 16 and 17) (points) and of Singh *et al.* (Ref. 18) (crosses).

Our interpretation concerning the origin of the  $U$  band in  $\text{CaF}_2$ ,  $\text{SrF}_2$ , and  $\text{BaF}_2$  is based on the fact that the most hydrogenlike orbital ( $3a_1$ ) lies well below the  $F^-$  bandlike states so that the calculated energy for the  $3a_1 - 7t_2$  transition is very large as compared to the experimental peak energy. One could think that the characteristics of the  $3a_1$  and  $4a_1$  orbitals are due to other features inherent to the  $\text{MSX}\alpha$  method or to the fact that possible relaxations of nearest neighbors were not considered. We then decided to test the sensibility of this result by varying the  $\alpha$  values and performing a calculation in a relaxed cluster; this check has only been made for the first cluster representation of the defect in  $\text{CaF}_2$ .

Figure 9 shows the uppermost electronic energy levels corresponding to four other calculations in which the same value of  $\alpha$  has been used for all the regions of the cluster. Concerning the values

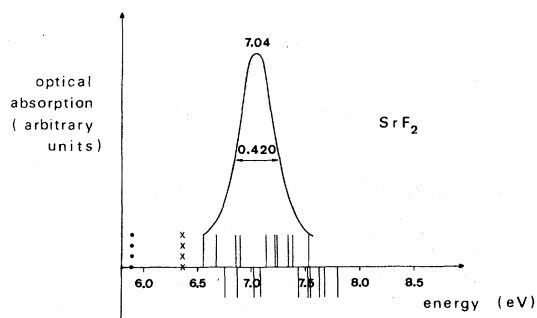


FIG. 7. Comparison between experiment and the results of the transition-state calculations for  $\text{SrF}_2$ . Vertical bars in the upper and lower sides of horizontal axis correspond to first- and second-cluster calculations, respectively. Also shown are the theoretical results of Bennett (Refs. 16 and 17) (points) and of Singh *et al.* (Ref. 18) (crosses).

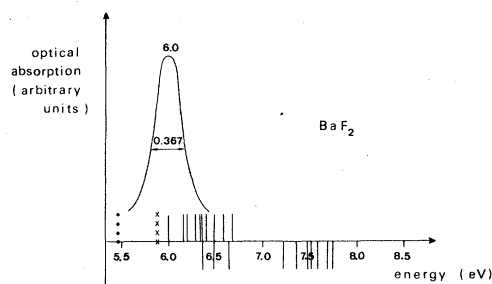


FIG. 8. Comparison between experiment and the results of the transition-state calculations for  $\text{BaF}_2$ . Vertical bars in the upper and lower sides of horizontal axis correspond to first- and second-cluster calculations, respectively. Also shown are the theoretical results of Bennett (Refs. 16 and 17) (points) and of Singh *et al.* (Ref. 18) (crosses).

of the transition energies, the only significant differences with respect to the  $\alpha$ -Schwarz calculation previously done are found in the cases of  $\alpha = 0.9$  and  $\alpha$ -Slater = 1.0; these differences amount to higher energy shifts of the order of 10% ( $\alpha = 0.9$ ) and 20% ( $\alpha$ -Slater = 1.0), on the average. Table X presents the percentual amount of charge inside the hydrogen and fluorine spheres arising from the wave function associated with the energy levels  $3a_1$  and  $4a_1$ , respectively. We can observe that the interchange of characteristics for these levels only occur for  $\alpha$ -Slater, which is well known to be an unrealistic choice for cluster calculations.

The calculation involving relaxation was performed by relaxing 6% inward the nearest neighbors, this amount being obtained in the variational method used by Bennett.<sup>16,17</sup> Our results for the uppermost energy levels are shown in Fig. 10. We verify once again that the ordering of the energy levels did not change. Also, the average shift of the transitions amounts to 3% in the lower energies direction and the characteristics of the  $3a_1$  and  $4a_1$  levels did not interchange [ $3a_1(\text{H}^-) = 85\%$  and  $4a_1(\text{F}^-) = 90\%$ ].

TABLE X. Percentual amount of charge inside the hydrogen and fluorine spheres arising from the wave functions associated with the energy levels  $3a_1$  and  $4a_1$  for  $\text{CaF}_2$  (first cluster) and different values of  $\alpha$  [ $\alpha$ -Gaspar (Ref. 38), Kohn and Sham (Ref. 39) ( $\alpha$ -GKS),  $\frac{2}{3}$ ;  $\alpha$ -Schwarz, commented in the text; and  $\alpha$ -Slater, 1.0].

	$\alpha$ -GKS	$\alpha$ -Schwarz	$\alpha = 0.80$	$\alpha = 0.90$	$\alpha$ -Slater
$3a_1(\text{H}^-)$	59%	61%	53%	47%	39%
$3a_1(\text{F}^-)$	28%	26%	34%	41%	51%
$4a_1(\text{H}^-)$	30%	28%	36%	43%	52%
$4a_1(\text{F}^-)$	64%	67%	59%	53%	44%

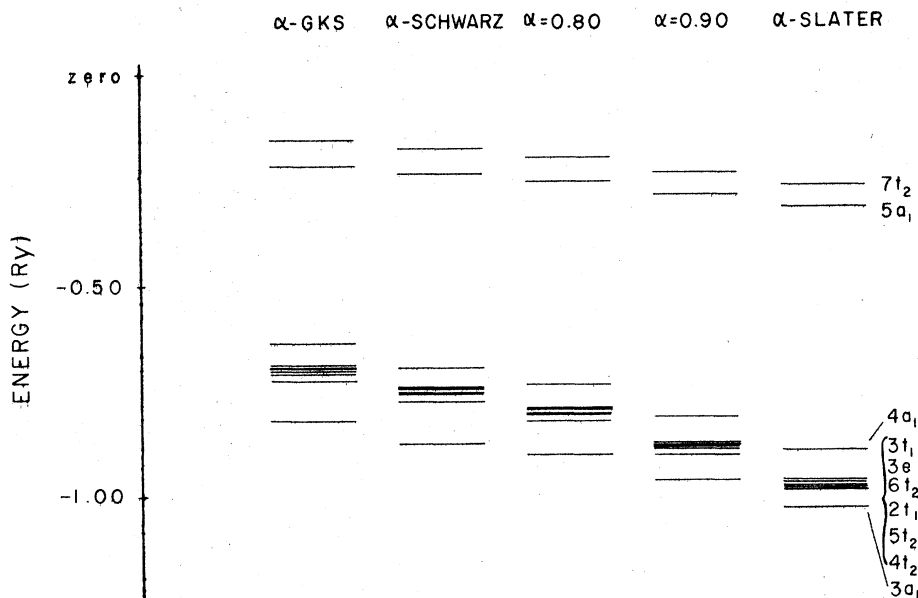


FIG. 9. One-electron energy levels from the ground-state calculation of the  $U$  center in  $\text{CaF}_2$  using the first cluster and different values of  $\alpha$  [ $\alpha$ -Gaspar (Ref. 38) Kohn and Sham (Ref. 39) ( $\alpha$ -GKS),  $\frac{2}{3}$ ].

#### IV. CONCLUSIONS

An important feature has been obtained from the present work. It concerns the character of the optical absorption  $U$  band in  $\text{CaF}_2$ ,  $\text{SrF}_2$ , and  $\text{BaF}_2$ , which as has been discussed in Sec. III B, cannot be associated with only a single  $\text{H}^-$  transition. This is contrary to all previously proposed models<sup>16-18</sup> and apparently distinguishes  $\text{CaF}_2$ ,

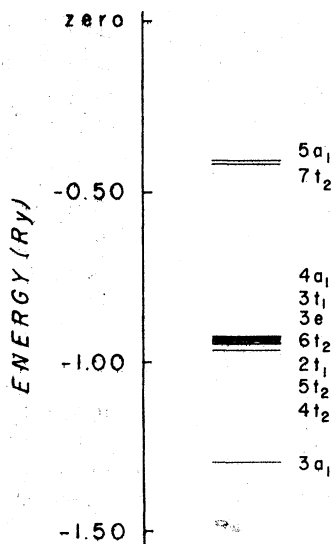


FIG. 10. One-electron energy levels from the ground-state calculation of the  $U$  center in  $\text{CaF}_2$  using the first cluster and relaxing the nearest neighbors.

$\text{SrF}_2$ , and  $\text{BaF}_2$  from the alkali halides. In these compounds the uppermost occupied level is in fact a hydrogenlike one and the optical transition seems to occur in  $\text{H}^-$ , as shown by Yu *et al.*<sup>20,21</sup> using the  $\text{MSX}\alpha$  method. Nevertheless, when the first shell of anions is included in the calculations, that hydrogenic level lies very close to the  $p$ -like anion levels; in such a case, it could be possible to associate the  $U$  band also with several transitions arising from these levels. In our calculations we have checked the characteristics of the  $3a_1$  and  $4a_1$  levels in several ways and showed their qualitative insensitiveness regarding different choices of parameters inherent to the  $\text{MSX}\alpha$  method.

The predictive character of the  $\text{MSX}\alpha$  method concerning the values of the transition energies also appeared to be satisfactory. Calculations using the first cluster representation for the defect gave results which lay reasonably inside the experimental band. Of course, the electron-phonon interaction and the calculation of relative oscillator strengths of the transitions should be considered to provide a more convincing picture of the results obtained, but this is beyond the scope of this paper. Polarization effects could in principle affect the quantitative results, but for such a noncharged and well localized defect (the charge inside  $\text{H}^-$  is always around  $2e^-$ ) our model does not predict significant changes; a calculation done for  $\text{CaF}_2$  using partial waves up to  $l=2$ , for the first and second shells, confirmed this feature.

Other good tests for the  $\text{MSX}\alpha$  method are the study of the  $F$  and  $U_3$  centers in these same compounds. This study is in progress.



- \*Work supported by Brazilian Agencies CAPES (Coordenação de Aperfeiçoamento do Pessoal de Ensino Superior), FINEP (Financiadora de Estudos e Projetos), and CNPq (Conselho Nacional de Desenvolvimento Científico e Tecnológico).
- <sup>1</sup>H. Dötsch and S. S. Mitra, *Phys. Rev.* **178**, 1492 (1969).  
<sup>2</sup>J. H. Schulman and W. Dale Compton, *Color Center in Solids* (Macmillan, New York, 1962).  
<sup>3</sup>M. V. Klein, in *Physics of Color Centers*, edited by W. Beall Fowler (Academic, New York, 1968).  
<sup>4</sup>R. Hilsch and R. Pohl, *Trans. Faraday Soc.* **34**, 883 (1938).  
<sup>5</sup>W. Martienssen, *Z. Phys.* **131**, 488 (1952).  
<sup>6</sup>G. Baldini, E. Mulazzi, and N. Terzi, *Phys. Rev.* **140**, A209 (1965).  
<sup>7</sup>S. S. Mitra and Y. Brada, *Phys. Rev.* **145**, 626 (1966).  
<sup>8</sup>W. Hayes and H. F. MacDonald, *Proc. R. Soc. Lond.* **A297**, 503 (1967).  
<sup>9</sup>R. J. Elliott, W. Hayes, G. D. Jones, H. F. MacDonald, and C. T. Sennett, *Proc. R. Soc. Lond. A* **289**, 1 (1966).  
<sup>10</sup>J. A. Harrington (unpublished).  
<sup>11</sup>J. H. Beaumont, J. V. Gee, and W. Hayes, *J. Phys. C* **3**, 152 (L) (1970).  
<sup>12</sup>B. S. Gourary, *Phys. Rev.* **112**, 337 (1958).  
<sup>13</sup>H. N. Spector, S. S. Mitra, and H. N. Schmeising, *J. Chem. Phys.* **46**, 2672 (1967).  
<sup>14</sup>R. F. Wood and U. Öpik, *Phys. Rev.* **162**, 736 (1967).  
<sup>15</sup>C. T. Sennett, *J. Phys. Chem. Solids* **26**, 1097 (1965).  
<sup>16</sup>H. S. Bennett, *Phys. Rev. B* **6**, 3936 (1972).  
<sup>17</sup>H. S. Bennett, *J. Res. Natl. Bur. Stand. A* **77**, 659 (1973).  
<sup>18</sup>R. S. Singh, D. W. Galipeau, and S. S. Mitra, *J. Chem. Phys.* **52**, 2341 (1970).  
<sup>19</sup>R. C. Chaney and C. C. Lin, *Phys. Rev. B* **13**, 843 (1976).  
<sup>20</sup>H. -L. Yu, Ph.D. thesis (University of Florida, 1975) (unpublished).  
<sup>21</sup>H. -L. Yu, M. L. de Siqueira, and J. W. D. Connolly, *Phys. Rev. B* **14**, 772 (1976).  
<sup>22</sup>E. Clementi, H. Kistenmacher, and H. Popkie, *J. Chem. Phys.* **58**, 4699 (1973).  
<sup>23</sup>K. H. Johnson, *J. Chem. Phys.* **45**, 3088 (1966).  
<sup>24</sup>J. C. Slater and K. H. Johnson, *Phys. Rev. B* **5**, 844 (1972).  
<sup>25</sup>K. H. Johnson, *Adv. Quantum Chem.* **7**, 143 (1973).  
<sup>26</sup>K. H. Johnson and F. C. Smith, *Chem. Phys. Lett.* **10**, 219 (1971).  
<sup>27</sup>J. W. D. Connolly and K. H. Johnson, *Chem. Phys. Lett.* **10**, 616 (1971).  
<sup>28</sup>J. W. D. Connolly, H. Siegbahn, U. Gelius, and C. Nordling, *J. Chem. Phys.* **58**, 4265 (1973).  
<sup>29</sup>L. Pauling, *The Nature of the Chemical Bond* (Cornell U.P., Ithaca, N. Y., 1948).  
<sup>30</sup>R. E. Watson, *Phys. Rev.* **111**, 1108 (1958).  
<sup>31</sup>J. C. Slater, *Phys. Rev.* **81**, 385 (1951).  
<sup>32</sup>J. C. Slater and J. H. Wood, *Int. J. Quantum Chem. Symp.* **4**, 3 (1971).  
<sup>33</sup>K. Schwarz, *Phys. Rev. B* **5**, 2466 (1972).  
<sup>34</sup>S. R. Singh and V. H. Smith, Jr., *Phys. Rev. A* **4**, 1774 (1971).  
<sup>35</sup>J. C. Slater, *Int. J. Quantum Chem. Symp.* **7**, 533 (1973).  
<sup>36</sup>J. C. Slater, *The Self-Consistent Field for Molecules and Solids* (McGraw-Hill, New York 1974).  
<sup>37</sup>*Inorganic Index to the Powder Diffraction File, American Society for Testing and Materials* (Joint Committee on Powder Diffraction Standards, Easton, Md., 1971).  
<sup>38</sup>R. Gaspar, *Acta Phys. Acad. Sci. Hung.* **3**, 263 (1954).  
<sup>39</sup>W. Kohn and L. J. Sham, *Phys. Rev.* **140**, A1133 (1965).